Int. J. Solids Structures Vol. 19, No. 7, pp. 587–599, 1983
Printed in Great Britain.

0020-7683/83 $3.00 + .00
Pergamon Press Ltd.

ON THE RATE-DEPENDENT ENDOCHRONIC THEORY OF VISCOPLASTICITY AND ITS APPLICATION TO PLASTIC-WAVE PROPAGATION

HSUAN-CHI LIN and HAN-CHIN WU†

Components Technology Division, Argonne National Laboratory, 9700 South Cass Avenue, Argonne, IL 60439, U.S.A.

(*Received* 8 *January* 1982; *in revised form* 1 *November* 1982)

Abstract—The constitutive equations for strain-hardening metallic materials with strain-rate effects are presented in the framework of the endochronic theory of viscoplasticity using the improved intrinsic time measure. The derived constitutive equations are then applied to the viscoplastic wave-propagation problem of a thin-walled tube subjected to impact loading. Numerical results using the improved endochronic time and theoretical results using conventional plasticity together with the experimental results are compared. It is shown that they are in good agreement qualitatively. In summary, the improved intrinsic time measure does predict both loading and unloading behavior in accordance with the observed phenomena.

NOTATION

c	wave speed
E_0	elastic modulus
E_1	material parameters
E_t	tangent modulus
i, j, k	indices
k_1	scalar number, $0 \leq k_1 \leq 1$
k_a, k_b	rate-sensitive material parameters
n, n_0	material parameters
P	fourth-order material tensor
Q	deviatoric part of r
r	stress-like function
t	time
u	velocity
x	spatial coordinate
z	endochronic time scale
$\alpha, \beta, \alpha_1, \beta_1$	endochronic material parameters
ϵ	small strain tensor
λ	heredity function
ρ	mass density
σ	stress tensor
ϕ, ψ	functions
σ_y	yield stress
σ_0	intercept of the asymptotic stress-strain curve at large strain with the stress axis
ζ	intrinsic time measure

1. INTRODUCTION

Intensive interest in the response of structural systems to extreme loads has led to the requirement of better understanding of material behavior beyond the elastic limit. In particular, for the purpose of structural integrity and reliability the design of the aerospace vehicular system and nuclear power plant facilities requires highly accurate knowledge of material behavior in the prediction of the dynamic system response. Further development of a viscoplasticity theory is needed to fulfill the requirements in those highly sophisticated structural systems. Traditionally, the flow theory of plasticity (or simply called classical plasticity in this report) has been widely employed by structural mechanicians. Classical plasticity, which forms the basis of virtually all theoretical models now in use in the general-purpose computer codes, requires that one traces the evolution of the material yield surface in the stress space and the location of the stress state of each point in a structure with respect to this surface. However, calculations relating to yield-surface evolution and logical checks of position on the yield surface are costly in computer time and storage requirements. A distinctive advantage of the endochronic theory proposed here is the potential savings in computer time.

†Division of Materials Engineering. The University of Iowa, Iowa City, IA 52242, U.S.A.

The endochronic theory of viscoplasticity initiated by Valanis[1] is based on the internal variable theory of irreversible thermodynamics together with the continuum-mechanics approach. The theory is an attempt to describe the material behavior over a wide spectrum of response using a unified constitutive equation such that the conventional elastic and inelastic behavior can be deduced from the general theory by suitable definitions of specific material parameters.

The original version of endochronic theory, the simple endochronic theory, has been applied to give analytic predictions for the quasi-static mechanical response of metallic[1–4] and nonmetallic[5–8] materials, the dynamic response of structures[9–15], and fracture mechanics and fatigue problems[16–19]. Although the simple endochronic theory can predict most of the observed mechanical behavior of materials, and it has been demonstrated[15] to save computer time in modeling the dynamic inelastic response of structural systems, it does show some discrepancies between experimental and theoretical predictions involving unloading behavior. Recently, Valanis[20] introduced a new measure of intrinsic time, which can eliminate or mitigate this deficiency, depending on the choice of a parameters and is more closely representative of the dissipation properties of material during unloading processes. As a consequence, the phenomenon of yield and the plastic strain are obtainable for a particular choice of the intrinsic time measure.

In the following, the general endochronic theory of viscoplasticity using the new intrinsic time measure is briefly summarized, a set of constitutive equations is obtained in differential form, and some numerical examples are presented using the new form of constitutive relationships to show the influence of various material parameters in the new formulation in terms of unloading–reloading behavior. Following the discussion of strain-rate effect on the dynamic behavior of metallic materials, such as α-titanium, the strain-rate-dependent constitutive equations are applied to investigate the viscoplastic wave-propagation problem related to a thin-walled tube subjected to an impulse loading.

2. CONSTITUTIVE EQUATIONS IN THE IMPROVED ENDOCHRONIC THEORY OF VISCOPLASTICITY

In the endochronic theory of viscoplasticity the history of deformation is defined in terms of a "time scale", which is not measured by a clock, but is in itself a property of the material at hand. An incremental time measure $d\zeta$ is defined such that

$$d\zeta^2 = P_{ijkl} d\epsilon_{ij} d\epsilon_{kl}, \tag{1}$$

where ϵ_{ij} is the strain tensor and P_{ijkl} is a positive definite material tensor. In addition, a time scale $z(\zeta)$ is introduced [1] such that $dz/d\zeta > 0$. The definition of intrinsic time in eqn (1) has led to difficulties in describing the material behavior involving unloading. Valanis [20] has since proposed an improved concept of intrinsic time to account for it. In the one-dimensional case the improved intrinsic time increment $d\zeta$ is defined as

$$d\zeta = \left| d\epsilon - k_1 \frac{d\sigma}{E_0} \right|, \tag{2}$$

where σ and ϵ are, respectively, the stress and strain; k_1 is a positive scalar such that $0 \geqslant k_1 \geqslant 1$; and E_0 is elastic modulus. When $k_1 = 0$, the improved intrinsic time reduces to the original definition of intrinsic time, and the theory is called simple endochronic theory. But when $k_1 = 1$, eqn (2) reduces to $d\zeta = d\epsilon - (d\sigma/E_0)$, which is the plastic-strain increment; thus the conventional concept of yield may be discussed within the framework of endochronic theory. It should be remarked that if the case of $k_1 = 1$ is believed to be representative of the metallic behavior, then by choosing k_1 to be close to 1, say, 0.95, an approximate representation may be achieved without having to introduce a discontinuity into the constitutive equation. This aspect is indeed a very important strength of the present approach.

For uniaxial stress, the improved endochronic constitutive equation is

$$\sigma = E_0 \int_0^z \lambda(z - z') \frac{dQ}{dz'} dz', \tag{3}$$

in which

$$E_0\lambda(z) = \frac{E_0}{1-k_1}e^{-\alpha_0/1-k_1 z} + E_1 e^{-\alpha z} \tag{4}$$

and

$$dQ = \left|d\epsilon - \frac{k_1}{E_0}d\sigma\right|, \tag{5}$$

where α_0, α, and E_1 are material parameters. The above equations have been derived for the case of two internal state variables. However, it has been shown [21] that this simple form is adequate for most of the cases considered. Furthermore, from eqns (3) and (4), we have

$$\sigma = \frac{E_0}{1-k_1}\int_0^z e^{-\alpha_0/1-k_1(z-z')}\frac{dQ}{dz'}dz + r, \tag{6}$$

and

$$r = E_1\int_0^z e^{-\alpha(z-z')}\frac{dQ}{dz'}dz'. \tag{7}$$

Equations (6) and (7) can be rewritten in a differential form as

$$\frac{1-k_1}{E_0}d(\sigma - r) + \frac{\alpha_0}{E_0}(\sigma - r)dz = dQ, \tag{8}$$

and

$$dr + \alpha r dz = E_1 dQ. \tag{9}$$

The differential form presented here is convenient for use in the numerical computation which will be demonstrated in this paper.

3. DETERMINATION OF MATERIAL PARAMETERS

The determination of the material constants appearing in the differential form will now be discussed. This can be done from test information for monotonic loading under constant strain rate. At this condition, it has been found in [21] that eqns (6) and (7) lead to

$$\sigma = \frac{E_0(1+\beta\zeta)}{\beta_1(n_0-k_1)}\{1-(1+\beta\zeta)^{-(n_0-k_1/1-k_1)}\} + \frac{E_1(1+\beta\zeta)}{\beta_1 n}\{1-(1+\beta\zeta)^{-n}\}, \tag{10}$$

where

$$n = \frac{\alpha}{\beta} + 1, \tag{11}$$

$$n_0 = \frac{\alpha_0}{\beta} + 1, \tag{12}$$

and

$$\beta_1 = \beta k. \tag{13}$$

In the derivation of the above equations, the intrinsic time was given by

$$d\zeta = k(\dot{Q})|dQ| \tag{14}$$

for strain-rate-sensitive materials[21, 22], where $k(\dot{Q})$ is a plastic strain-rate-dependent function and may be found from experimental stress–strain curves at various constant strain rates. The hardening function which provides a scaling to the intrinsic time was given[1] by

$$\frac{d\zeta}{dz} = 1 + \beta\zeta, \tag{15}$$

in which β is a material parameter.

Some additional relations between certain quantities and constants may be found from loading represented by eqn (10). From the definition of the improved intrinsic time (eqn 2) with $k_1 = 1$, at the initiation of intrinsic time measure $\zeta = 0_+$ (i.e. when $Q = Q_+$), σ is equal to the yield stress. Thus, eqn (10) reduced to

$$\sigma_y = \frac{E_0}{\beta_1(n_0 - 1)}. \tag{16}$$

For large ζ (or Q), eqn (10) approaches an asymptotic line given by

$$\sigma = \sigma_y(1 + \beta_1 Q) + \frac{E_1}{\beta_1 n}(1 + \beta_1 Q). \tag{17}$$

Defining σ_0 as the intercept of this asymptotic line with the stress axis and E_t, the tangent modulus of the asymptotic line, it is possible to establish [21] that

$$\frac{E_1}{\beta_1 n} = \sigma_0 - \sigma_y \tag{18}$$

and

$$\beta_1 = \frac{E_t}{\sigma_0}. \tag{19}$$

Combining eqns (10), (16), (18) and (19), for $k_1 = 1$, the constitutive equations may be written in the following simple form:

$$\sigma = (1 + \beta_1 Q)[\sigma_0 - (\sigma_0 - \sigma_y)(1 + \beta_1 Q)^{-n}]. \tag{20}$$

The material constants, E_0, E_t, σ_0 and σ_y, can be measured directly from each constant strain-rate stress–strain curve. Then, β_1 may be determined from eqn (19). For a strain rate the same as the reference strain rate, $\beta_1 = \beta$ is obtained. Equation (20) may then be used to fit the experimental data by a trial-and-error procedure. The parameter n can thus be determined. Finally, eqns (16) and (18) can be used to determine n_0 and E_1. The parameters α and α_0 can also be obtained from eqns (11) and (12).

4. LOADING-UNLOADING-RELOADING RESPONSES

To demonstrate the consequence of the improved intrinsic time ζ on the behavior of loading–unloading for metallic materials, eqns (8), (9), (14) and (15) may be rewritten in the following form, making use of eqn (2):

$$\left(\frac{1 - k_1}{E_0}\right)d\sigma - \left(\frac{1 - k_1}{E_0}\right)dr - \left[1 \mp \frac{k\alpha_0(\sigma - r)}{E_0(1 + \beta\zeta)}\right]dQ = 0, \tag{21}$$

$$dr - \left[E \mp \frac{k\alpha r}{1 + \beta\zeta}\right]dQ = 0, \tag{22}$$

and

$$\left(\frac{k_1}{E_0}\right)d\sigma + dQ = d\epsilon. \tag{23}$$

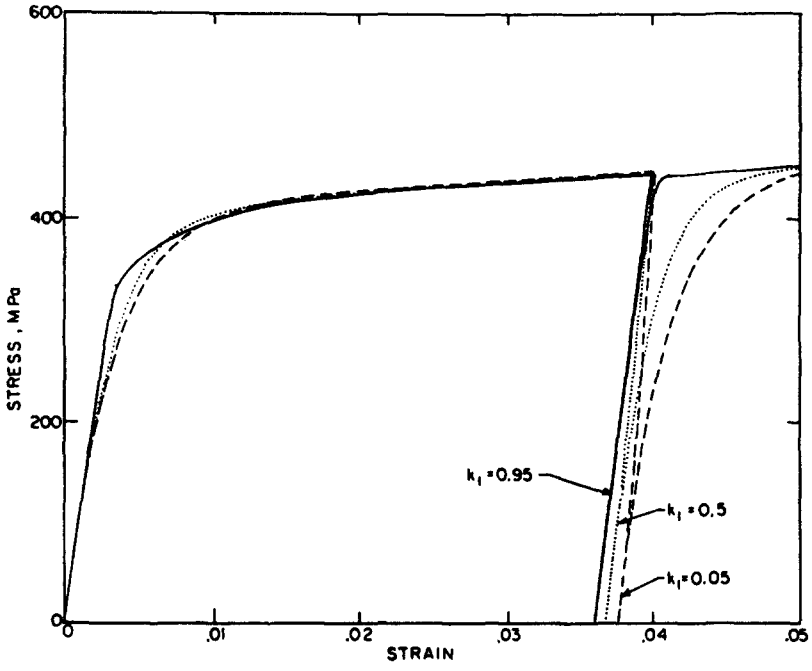

Fig. 1. Loading-unloading behavior of various k_1 values for α-Ti.

The above set of constitutive equations is valid for the uniaxial stress case. The negative sign is for the case of positive strain increment and the positive sign for negative strain increment. *All the material parameters involved can be determined following the discussion presented in the previous section.* To show the influence of parameter k_1, a set of stress-strain curves for α-titanium is presented in Fig. 1 for $k_1 = 0.05$, 0.5 and 0.95. For $k_1 = 0.05$, it can be seen that the unloading–reloading behavior is of the type of simple endochronic; for $k_1 = 0.95$, the unloading–reloading behavior approaches the elastic behavior. For $k_1 = 1$, the unloading–reloading curve is a straight line, and a distinct yield point is predicted. Therefore, it is seen that the theory with improved endochronic time can reasonably describe the elastic–plastic unloading–reloading and yield phenomena and that the case of $k_1 = 0.95$ provides a good approximation of this behavior.

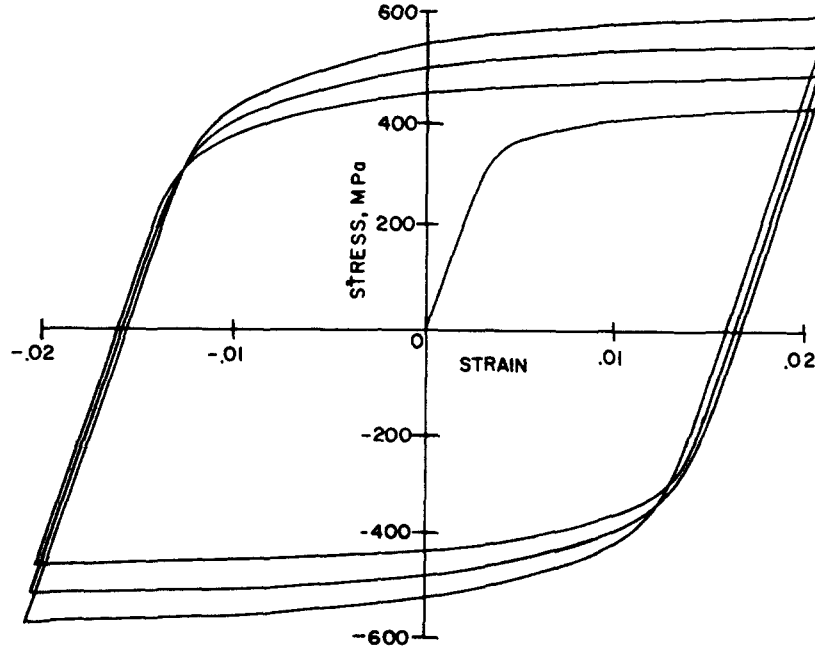

Fig. 2. Cyclic hardening behavior of α-Ti.

More figures present the theoretical unloading and reverse-loading behavior for α-titanium with unloading to various strains ranging from positive to negative values, respectively, can be found in [36]. These figures clearly show the formation of loading-unloading loops as observed in the experiments. Figure 2 presents the results of strain-controlled cyclic behavior of α-titanium for the first three cycles. Here again, the improved endochronic theory provides a reasonable description of material behavior. The endochronic description of cyclic behavior of metallic materials was previously discussed by Wu and Yip[22] using the finite form of the endochronic constitutive equation. In this computation, it is shown that this can also be achieved by use of the differential form given by eqns (21)–(23).

5. STRAIN-RATE EFFECT IN THE ENDOCHRONIC THEORY OF VISCOPLASTICITY

The influence of strain rate on the mechanical response of materials has been studied extensively in the past. It is clear that many practical dynamic problems such as crack propagation in ductile materials, stress-wave propagation, and high-rate metal-forming processes can be treated satisfactorily if the rate dependence of plastic material behavior is considered. An observation from experiments of plastic-wave propagation in tubes or rods[23–28] concluded that the mechanical behavior of strain-rate-sensitive materials cannot be described by a single stress–strain curve, but may be explained by a set of curves each corresponding to a specific strain rate. Various constitutive equations have been proposed in the past to accommodate the strain-rate effect. Most of them, based on the observed phenomenon, have assumed that the plastic rate of strain is a function of the dynamic overstress ([29–31], *et al.*). Critescu[32] subsequently generalized the idea into a full quasi-linear constitutive equation as follows:

$$\frac{\partial \epsilon}{\partial t} = \Phi(\sigma, \epsilon)\frac{\partial \sigma}{\partial t} + \Psi(\sigma, \epsilon), \tag{24}$$

where the functions Ψ and Φ represent, respectively, the noninstantaneous and the instantaneous response of the material to the increment of stress σ, and t is the time. Note that this equation does not account for the dependence of the material behavior on the strain-rate history. Many researchers, such as Klepaczko[33], and Senseny *et al.*[34], have shown that the strain-rate history effect can play a very important role in the wave-propagation problems. More discussion on the strain rate and strain-rate history effects can be found in [12, 21].

In the improved endochronic theory, the values of σ_0 and σ_y (in eqns 16 and 18) are functions of strain rate. Thus, for each strain rate, there is a corresponding stress–plastic strain curve. As indicated in [12, 21] assuming k of eqn (14) to be equal to 1 on the curve of reference strain rate, i.e. $\dot{Q} = \dot{Q}_0$, the following expression for the k function can describe the dynamic stress–strain curve of α-titanium nicely for strain rates ranging from 10^{-5} to $10^{-2}\,s^{-1}$.

$$k(\dot{Q}) = 1 - k_a \log\left(\frac{\dot{Q}}{\dot{Q}_0}\right), \tag{25}$$

where k_a is a strain-rate-sensitive parameter and can be determined following the procedures described in [12]; and $\dot{Q}_0$ is a reference strain rate, which is conveniently chosen. Note that for a different value of $\dot{Q}_0$, k_a needs to be modified accordingly. Figure 3 presents the results of three-stepped change of strain rate. Loading from the virgin state at $\dot{Q}_1 = 2\times10^{-4}\,s^{-1}$ up to $\epsilon = 0.025$. The $\dot{Q}$ then drops to $\dot{Q}_0 = 2\times10^{-5}\,s^{-1}$, while the loading continues until $\epsilon = 0.032$, at which time the strain rate suddenly jumps to $\dot{Q}_2 = 8\times10^{-4}\,s^{-1}$ for a while and then back to the initial strain rate $\dot{Q}_1 = 2\times10^{-4}\,s^{-1}$. The figure also shows the stress-strain curves at three different constant strain rates (dash, chain-dash, and dot lines). The experimental curves of reference strain rate (same as dot line) are taken from [35]; it can be seen that the agreement between predicted and experimental results is excellent. As indicated in Fig. 3, the change from lower strain rate to higher strain rate would cause the stress level to increase gradually from the lower constant strain-rate curve to the higher-strain-rate curve; the change from higher strain rate to lower strain rate is almost instantaneous. Note that due to small change in the range of

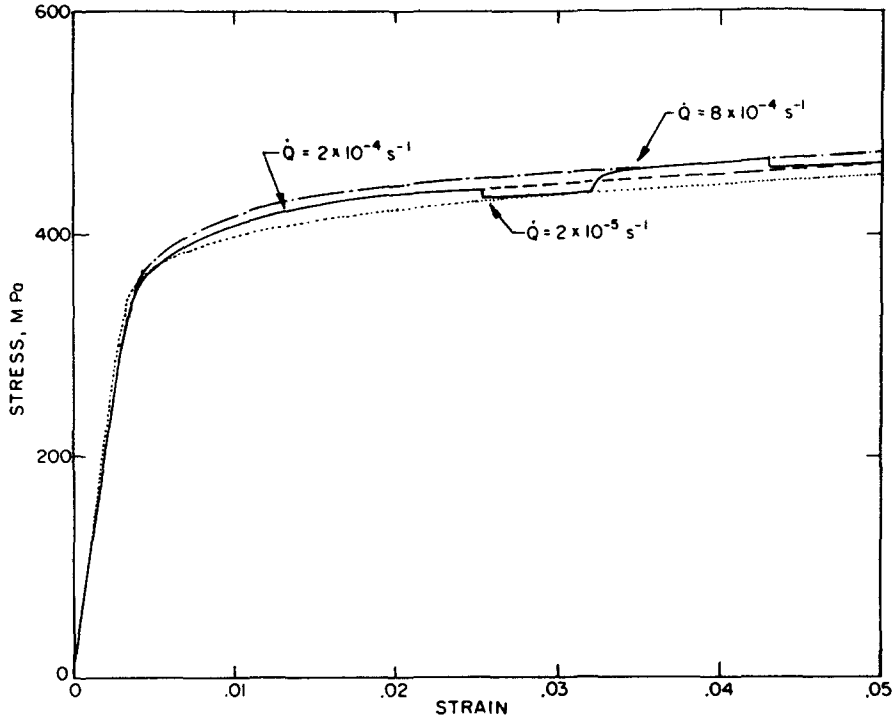

Fig. 3. Three-stepped change of strain rate for α-Ti.

strain rate, the elastic response in the low to high strain rate change is not obvious in this figure as reported in [21].

For more decades of the strain-rate range, the linear function of eqn (25) is not adequate in representing the entire spectrum for α-titanium. Therefore, a higher-order term must be used. A quadratic form of strain-rate function is proposed to describe the strain rate ranging from 10^{-5} to $10^{3}\ s^{-1}$ as follows:

$$k(\dot{Q}) = 1 - k_a \log\left(\frac{\dot{Q}}{\dot{Q}_0}\right) - k_b\left(\log\frac{\dot{Q}}{\dot{Q}_0}\right)^2, \tag{26}$$

where, k_b is the second-order strain-rate-sensitive parameter. Figure 4 presents the stress–strain

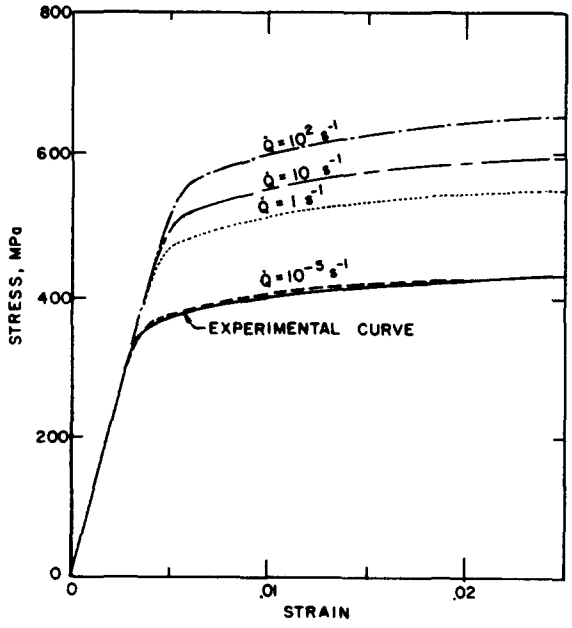

Fig. 4. Stress–strain curves of α-Ti for various constant strain rates.

curves of α-titanium at constant strain rate ranging from 2×10^{-5} to 10^2 s^{-1} using eqn (26). The values of k_a and k_b are obtained by fitting eqn (26) through data points in [35]. The material constants used in the present calculation for α-titanium are as follows:

$E_0 = 110$ GPa, $E_t = 0.413$ GPa, $\sigma_y = 0.351$ GPa, $\sigma_0 = 0.42$ GPa, $n = 200$, $\rho = 4.52 \times 10^3$ kg/m^3, $k_a = 0.04$, and $k_b = 0.002$. Hence, it is found that the quadratic function of strain-rate sensitivity can predict adequate dynamic stress–strain curves over a large range of strain rates in α-titanium.

6. VISCOPLASTIC WAVE PROPAGATION UNDER UNIAXIAL STRESS

To show the influence of strain rate on the dynamic material response using the improved endochronic time, the problem of longitudinal wave propagation in thin rods will be studied as an example. Let an elastic hitter impact on a semi-infinite long α-titanium slender, thin-walled tube through a transmitter. The constitutive equation for the uniaxial stress with strain-rate effect as derived in the previous section can be written as

$$\sigma_t - \left\{ \frac{1}{\left[E_1 \mp \dfrac{k\alpha r}{1+\beta\zeta}\right] + \dfrac{1}{1-k_1}\left[E_0 \mp \dfrac{k\alpha_0(\sigma - r)}{1+\beta\zeta}\right]} + \frac{k_1}{E_0} \right\}^{-1} \epsilon_t = 0. \tag{27}$$

Equation (27) was arrived by substituting eqns (22) and (23) into eqn (21). The equation of motion and the compatibility condition are

$$\sigma_x + \rho u_t = 0 \tag{28}$$

and

$$\epsilon_t + u_x = 0, \tag{29}$$

where u is the longitudinal particle velocity, x is the distance from the impact end of the rod to the cross section under consideration. Subscripts x and t denote the partial differentiation with respect to the corresponding variable. Compressive stress, compressive strain, and velocity in the positive x direction are taken to be positive.

Equations (27)–(29) comprise a system of equations for three explicit variables, σ, ϵ, and u, and four implicit functions, k, ζ, r, and Q, which can be found from constitutive equations derived previously. Numerical solutions were obtained for the above set of equations by means of the method of characteristics using a rectangular mesh similar to that in [35]. During calculation, the strain rate was considered constant for each small time increment, and the following characteristics were used to obtain the numerical solution for the system of eqns (27)–(29):

$$\frac{dx}{dt} = \pm c \tag{30}$$

and

$$dx = 0, \tag{31}$$

where

$$c = \sqrt{\frac{1}{\rho}\left\{ \frac{1}{\left[E_1 \mp \dfrac{k\alpha r}{1+\beta\zeta}\right] + \dfrac{1}{1-k_1}\left[E_0 \mp \dfrac{k\alpha_0(\sigma - r)}{1+\beta\zeta}\right]} + \frac{k_1}{E_0} \right\}^{-1}}. \tag{32}$$

The corresponding differential equations along the characteristics for this numerical procedures are

$$d\sigma \pm \rho c\, du = 0; \text{ on } \frac{dx}{dt} = \pm c; \tag{33}$$

and

$$d\sigma - \rho c^2 d\epsilon = 0; \text{ on } dx = 0. \tag{34}$$

The upper and lower signs in eqn (33) correspond to each other.

The velocity boundary condition was assumed to be of a smooth transition consisting of two parabolic segments during the period of rise time similar to that used by Hsu and Clifton[35], i.e.

$$u(0, t) = 0.5u_0\left[1 + \left(\frac{t}{t_h} - 1\right)\left(2 - \left|\frac{t}{t_h} - 1\right|\right)\right], \tag{35}$$

where u_0 is the prescribed constant value of u after the rise time, and t_h is one-half of the rise time. For t greater than the rise time, the velocity $u(0, t)$ is assumed to remain constant until unloading begins. At this time the longitudinal stress $\sigma(0, t)$ is taken to decrease to zero along a curve of the form of eqn (35). The corresponding change in the velocity $u(0, t)$ is such that longitudinal separation of the transmitter and specimen would result.

Experimental and theoretical work of the aforementioned problem has been studied by Hsu and Clifton[35]. The theoretical work in [35] was carried out using elastoplastic flow theory with the dynamic overstress derived from dislocation theory.

The numerical results using the improved endochronic time and theoretical and experimental results of [35] are compared in Fig. 5 in terms of strain-time profiles for $u_0 = 37.34$ m/s. All the material parameters involved were determined from the set of constant strain rate curves presented in Fig. 4 using the procedures described in Section III. The values of these material constants are given in the paragraph following eqn (26). The qualitative features of the computed and experimental profiles are in good agreement. As indicated in [35], neither the experiment nor the computed profiles show the steep, low-velocity plastic wave front or the plateau of uniform strain that would be expected from a rate-independent theory or from experiments on a less rate-sensitive material such as aluminum. The major discrepancy between computed and measured strain-time profiles is that the precursor decay in the former is considerably slower than that in the latter. This discrepancy exists on both results using endochronic and flow theory. However, there is a consistant difference between endochronic and flow theory; i.e. the endochronic strain-time profiles seems to be parallel to the experimental results, although they are always on the higher side while the flow-theory prediction has a tendency to cross over the experimental curves.

The computed dynamic stress–strain curves and the stress-time profiles at various locations

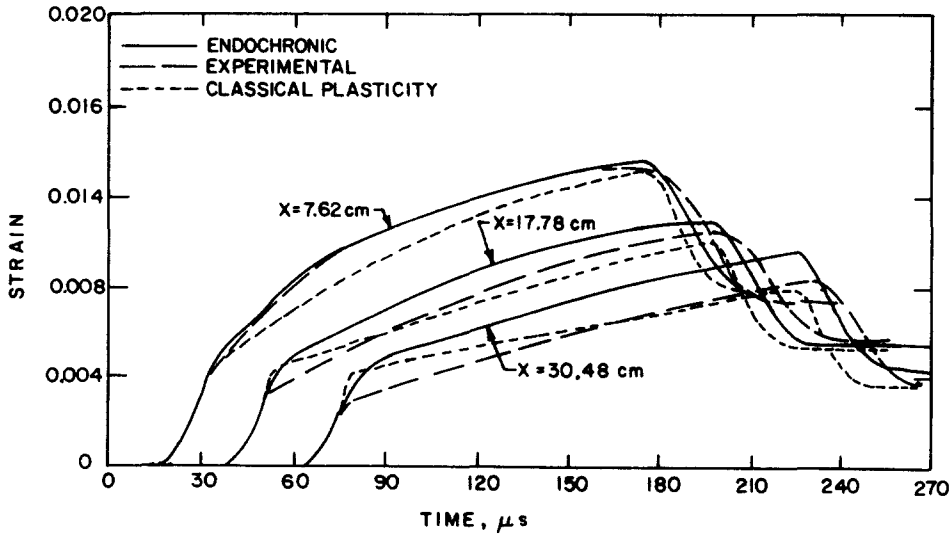

Fig. 5. Strain-time histories of longitudinal waves in α-Ti, ($u_0 = 37.34$ m/s).

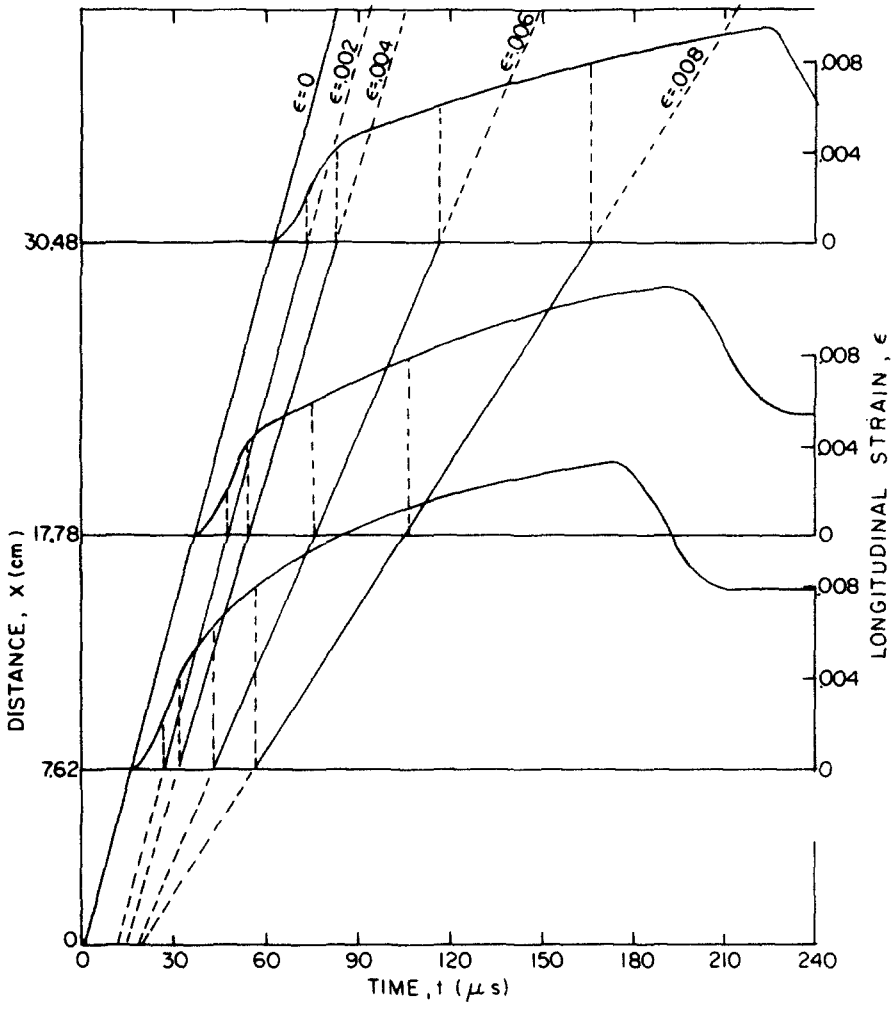

Fig. 6. Contours of constant strain in the x–t plane for α-Ti ($u_0 = 37.34$ m/s).

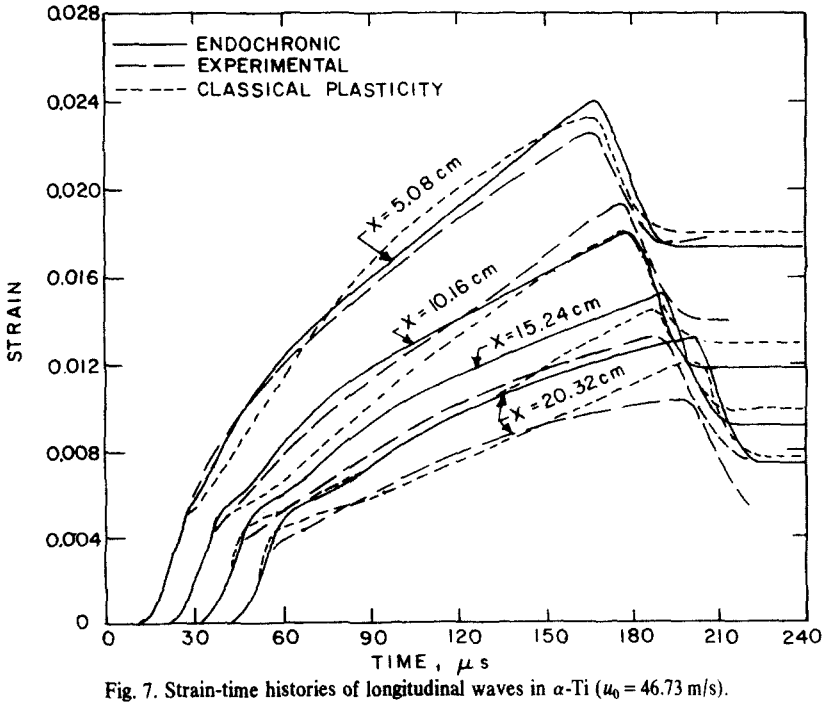

Fig. 7. Strain-time histories of longitudinal waves in α-Ti ($u_0 = 46.73$ m/s).

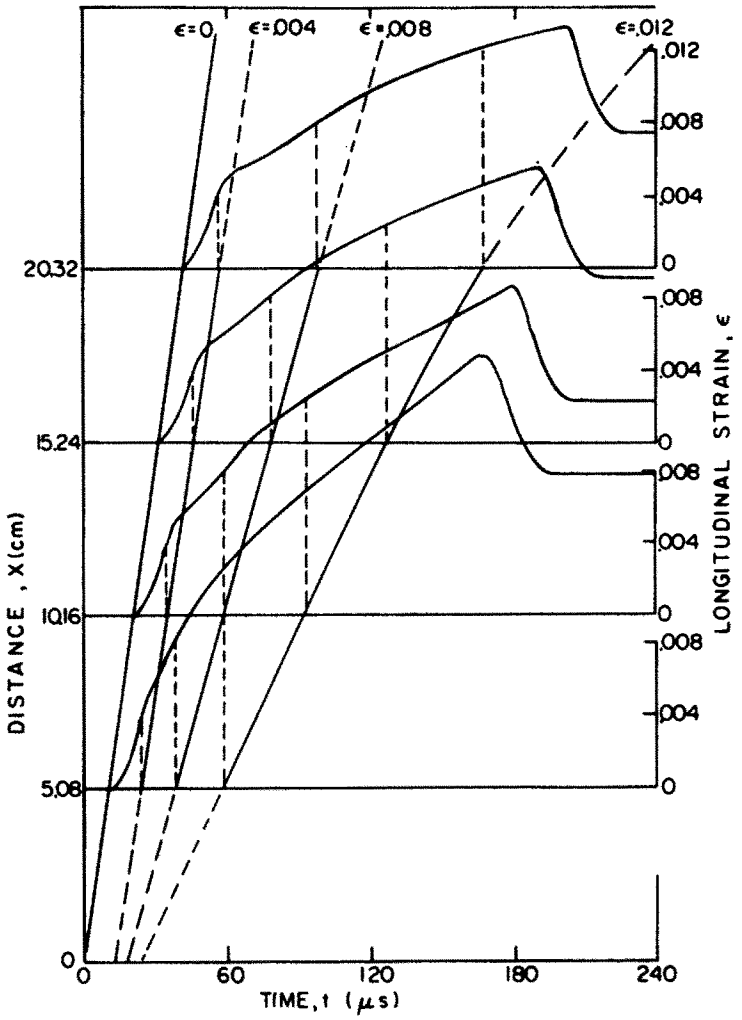

Fig. 8. Contours of constant strain in the x–t plane for α-Ti ($u_0 = 46.73$ m/s).

[36] also show the influence of rate sensitivity on the wave profiles. The stress level in the wave is clearly well above the level in quasi-static tensile tests at the same values of strain. Figure 6 presents the computed longitudinal-wave profiles and contours of constant strain in the x–t plane for α-titanium with $u_0 = 37.34$ m/s. As can be seen from the figure, the contours of the constant strain almost behave as a straight line similar to the simple wave solution, at least in the region near the impact end.

Figures 7 and 8 present similar results for α-titanium with $u_0 = 46.73$ m/s. It seems that all the observations in the case of $u_0 = 37.34$ m/s apply to the latter case. However, it is noted that in the Fig. 8, the contours of the constant strain begins to deviate from straight line for ϵ equals 0.012. Thus the attenuation of wave profiles begins to appear for larger plastic strain. Comparisons between computed and experimental results in the unloading region are all in good agreement qualitatively (see Figs. 5 and 7), although computed values using endochronic theory are consistently higher than the experimental results at larger x. The results demonstrate that the improved intrinsic time formulation can predict much better unloading behavior than the simple endochronic theory.

7. CONCLUDING REMARKS

It has been shown that the differential endochronic constitutive equations derived in this report can be used to describe the uniaxial stress behavior of α-titanium subject to loading-unloading-reloading cycles. The effects of strain rate and its history have been investigated. Furthermore, these differential constitutive equations have been applied to the study of

viscoplastic wave propagation in a thin-walled tube subjected to impact loading. The theoretical results have been compared with both the experimental results and the results of flow theory of plasticity found in the literature.

The differential endochronic constitutive equations used in the computation are based on the improved endochronic time. The parameter k_1 defined by the improved endochronic time has been found to play an important role in the numerical computation. For $k_1 \neq 1$, no discontinuity is built into the constitutive equation, and thus the advantage found in the computation using the simple endochronic theory is preserved. It has been found that a value of $k_1 = 0.95$ would provide a good approximation.

Acknowledgements—We are grateful to Drs. C. A. Kot and G. S. Rosenberg for valuable suggestions and comments. The support by Dr. Oscar Manley, Office of Basic Energy Sciences, U.S. Department of Energy, is greatly appreciated.

REFERENCES

1. K. C. Valanis, A theory of viscoplasticity without a yield surface—I: General theory—II. Application to mechanical behavior of metal. *Arch. Mech. Stosow.* **23**, 517–551 (1971).
2. K. C. Valanis, Effect of prior deformation of cyclic response of metals. *J. Appl. Mech.* **41**, 441–447 (1974).
3. K. C. Valanis and H. C. Wu, Endochronic representation on cyclic creep and relaxation of metals. *J. Appl. Mech.* **42**, 67–73 (1975).
4. G. Wempner and J. Aberson, A formulation of inelasticity from thermal and mechanical concepts. *Int. J. Solid Structures* **12**, 705 (1976).
5. Z. P. Bazant and P. Bhat, Endochronic theory in inelasticity and failure of concrete. *J. Engng Mech. Div., ASCE* **102**, 701–722 (1976).
6. Z. P. Bazant and R. J. Krizek, Endochronic constitutive law for liquefaction of sand. *J. Engng Mech. Div., ASCE* **102**, 225–238 (1976).
7. Z. P. Bazant, P. Bhat and C. L. Shieh, Endochronic theory for inelasticity and failure analysis of concrete structures. Structural Engineering Rep. 1976–12/259 Northwestern University, Dec. 1976, to Oak Ridge National Laboratory (ORNL/SUB/4403–1).
8. I. P. DeVilliers, Implementation of endochronic theory for analysis of concrete structures. Ph.D. Thesis, University of California, Berkeley (1977).
9. H. C. Wu and H. C. Lin, Plastic waves in a thin-walled tube under combined longitudinal and torsional loads. *10th Anniversary Meeting*, Society of Engineering Science, North Carolina State University (Nov. 1973).
10. H. C. Wu and H. C. Lin, Combined plastic waves in a thin-walled tube. *Int. J. Solids Struct.* **10**, 903–917 (1974).
11. H. C. Wu and H. C. Lin, Combined plastic waves in a thin-walled tube. 7th U.S. Nat. Cong. Appl. Mech., University of Colorado (June 1974).
12. H. C. Lin and H. C. Wu, Strain-rate effect in the endochronic theory of viscoplasticity. *J. Appl. Mech.* **98**, 92–96 (1976).
13. H. C. Lin, Dynamic plastic deformation of axi-symmetric circular cylindrical shells. *Nucl. Engng Des.* **35**, 283–293 (1975).
14. H. C. Lin, Dynamic inelastic response of thick shells using endochronic theory and the method of nearcharacteristics. *13th Ann. Meeting*, Society of Engineering Science, NASA CP-2001, 2, PP. 449–458. (1976).
15. H. C. Lin, B. J. Hsieh and R. A. Valentin, The application of endochronic plasticity theory in modeling the dynamic inelastic response of structural systems. *Nucl. Engng Des.* **66**, 213–222 (1981).
16. H. C. Lin, Axial crack propagation in a pressurized pipe due to ductile failure. *8th U.S. Nat. Cong. Appl. Mech.* UCLA (June 1978).
17. H. C. Lin, Dynamic propagation of longitudinal cracks in a pressurized cylindrical shell due to ductile failure. *Nucl. Engng Des.* **63**, 137–142 (1981).
18. K. C. Valanis, An energy-probability theory of fracture. *J. Mec.* **14**, 843–862 (1975).
19. K. C. Valanis and H. C. Wu, Fracture of plastic materials under proportional straining—I. Theoretical foundations—II. Application to gray cost iron. *J. Méc.* **15**, 543–577 (1976).
20. K. C. Valanis, Fundamental consequences of a new intrinsic time measure-plasticity as a limit of the endochronic theory. *Arch. Mech.* **32**, 171–191 (1980).
21. H. C. Wu and M. C. Yip, Strain-rate and strain-rate history effects on the dynamic behavior of metallic materials. *Int. J. Solids Structures* **16**, 515–536 (1980).
22. H. C. Wu and M. C. Yip, Endochronic description of cyclic hardening behavior for metallic materials. *J. Engng Mater. Technol., Trans. ASME* **103**, 212–217 (1981).
23. J. F. Bell, Propagation of large amplitude waves in annealed aluminum. *J. Appl. Phys.* 31, 277–282 (1960).
24. J. F. Bell, The physics of large deformation of crystalline solids. *Springer Tracts in Natural Philosophy*, Vol. 14. Springer-Verlag, Berlin (1968).
25. H. Kolsky and L. S. Douch, Experimental studies in plastic wave propagation. *J. Mech. Phys. Solids* **10**, 195–223 (1962).
26. O. W. Dillon, Jr., Experimental data on small-plastic deformation waves in annealed aluminum. *Int. J. Solids Structures* **4**, 197–223 (1968).
27. L. Efron and L. E. Malvern, Electromagnetic velocity-transducer studies of plastic wave in aluminum bars. *Exp. Mech.* **9**, 255–262 (1969).
28. C. H. Yew and H. A. Richardson Jr., The strain-rate effect and the incremental plastic wave in copper. *Exp. Mech.* **9**, 366–373 (1969).
29. L. E. Malvern, The propagation of longitudinal waves of plastic deformation in a bar of material exhibiting a strain-rate effect. *J. Appl. Mech.* **18**, 203–208 (1951).
30. V. V. Sokolovskii, The propagation on elastic viscoplastic waves in bars. *Prikl. Mat. Mek.* **12**, 261–280 (1948).
31. P. Perzyna, The constitutive equations for rate-sensitive materials. *Q. Appl. Math.* **20**, 321–332 (1963).

32. N. Cristescu, *Dynamic Plasticity*. North Holland, Amsterdam (1967).
33. J. Klepaczko, Strain-rate history effects for polycrystalline aluminum and theory of intersections. *J. Mech. Phys. Solids* **16**, 255–266 (1968).
34. P. E. Senseny, J. Duffy and R. H. Hawley, Experiments on strain rate history and temperature effects during the plastic deformation of close packed metals. *J. Appl. Mech.* **45**, 60–66 (1978).
35. J. C. C. Hsu and R. J. Clifton, Plastic waves in a rate sensitive material—I: waves of uniaxial stress. *J. Mech. Phys. Solids* **22**, 233–253 (1974).
36. H. C. Lin and H. C. Wu, On the improved endochronic theory of viscoplasticity and its application to plastic-wave propagation. Argonne Nat. Lab. Rep., ANL-CT-81-37 (1981).